



HHS Public Access

Author manuscript

Eur J Nucl Med Mol Imaging. Author manuscript; available in PMC 2020 January 01.

Published in final edited form as:

Eur J Nucl Med Mol Imaging. 2019 January ; 46(1): 148–158. doi:10.1007/s00259-018-4096-y.

First-in-Human Study of ^{177}Lu -EB-PSMA-617 in Patients with Metastatic Castration-Resistant Prostate Cancer

Jie Zang^{1,2}, Xingrong Fan³, Hao Wang^{1,2}, Qingxing Liu^{1,2}, Jingnan Wang^{1,2}, Hui Li^{1,2}, Fang Li^{1,2}, Orit Jacobson⁴, Gang Niu⁴, Zhaohui Zhu^{1,2}, and Xiaoyuan Chen⁴

¹Department of Nuclear Medicine, Peking Union Medical College (PUMC) Hospital, Chinese Academy of Medical Science and PUMC, Beijing 100730, China

²Beijing Key Laboratory of Molecular Targeted Diagnosis and Therapy in Nuclear Medicine, Beijing 100730, China

³Department of Urology, Peking Union Medical College (PUMC) Hospital, Chinese Academy of Medical Science and PUMC, Beijing 100730, China

⁴Laboratory of Molecular Imaging and Nanomedicine (LOMIN), National Institute of Biomedical Imaging and Bioengineering (NIBIB), National Institutes of Health (NIH), Bethesda, Maryland, 20892, USA

Abstract

Purpose: This translational study is designed to assess the safety, dosimetry and therapeutic response to a single, low-dose of ^{177}Lu -EB-PSMA-617 in comparison to ^{177}Lu -PSMA-617 in patients with mCRPC.

Methods: Following institutional review board approval and informed consent, 9 patients with mCRPC were recruited. Four patients accepted intravenous injection of 0.80–1.1 GBq (21.5–30 mCi) of ^{177}Lu -EB-PSMA-617, then underwent serial whole-body planar and SPECT/CT imaging at 2, 24, 72, 120 and 168 h. The other 5 patients accepted intravenous injection of 1.30–1.42 GBq (35–38.4 mCi) ^{177}Lu -PSMA-617, then underwent the same imaging procedures at 0.5, 2, 24, 48, and 72 h. All patients were evaluated by ^{68}Ga -PSMA-617 PET/CT before and one month after the treatment. Dosimetry evaluation was compared in both patient groups.

Results: When the bone metastasis tumors with comparable baseline SUV_{max} in the range of 10.0–15.0 were selected from the two groups for comparison, the accumulated radioactivity of ^{177}Lu -EB-PSMA-617 was about 3.02-fold higher than that of ^{177}Lu -PSMA-617. Imaging dose of ^{177}Lu -EB-PSMA-617 treatment showed significant decrease of ^{68}Ga -PSMA-617 uptake within a month, which was not observed in patients imaged with ^{177}Lu -PSMA-617 (SUV change: $-32.43 \pm 0.14\%$ vs. $0.21 \pm 0.37\%$; $P = 0.002$). ^{177}Lu -EB-PSMA-617 also had higher absorbed doses in the red bone marrow and kidneys than ^{177}Lu -PSMA-617 (0.0547 ± 0.0062 vs. 0.0084 ± 0.0057

Compliance with Ethical Standards

Conflict of Interest: The authors declare that they have no conflict of interest.

Ethical approval: All procedures performed in studies involving human participants were in accordance with the ethical standards of the institutional and/or national research committee and with the 1964 Helsinki declaration and its later amendments or comparable ethical standards.

mSv/MBq for red bone marrow, $P < 0.01$; 2.39 ± 0.69 vs. 0.39 ± 0.06 mSv/MBq for kidneys, $P < 0.01$).

Conclusion: This first-in-human study demonstrated that ^{177}Lu -EB-PSMA-617 had higher accumulation in mCRPC and that low imaging dose appears to be effective in treating tumors with high ^{68}Ga -PSMA-617 uptakes. Elevated uptakes of ^{177}Lu -EB-PSMA-617 in kidneys and red bone marrow were well tolerated at the administered low dose. Further investigations with increased dose and frequency of administration are warranted.

Keywords

radioligand therapy (RLT); ^{177}Lu ; Evans blue; prostate-specific membrane antigen (PSMA); metastatic castration-resistant prostate cancer (mCRPC)

INTRODUCTION

Prostate cancer (PC) is the second most common cancer worldwide in men, with persistently high numbers dying from this disease [1]. Metastatic spread and disease progression under androgen deprivation therapy define the onset of metastatic castration resistant prostate cancer (mCRPC), the lethal form of the disease [2]. Despite recent advances in the treatment of mCRPC such as the androgen-receptor antagonist enzalutamide and the CYP17A1-inhibitor abiraterone, resistance to these treatments occurs frequently within 1 to 2 years [3]. The disease eventually progresses and patients survive less than 20 months [4]. For this reason, a targeted radionuclide approach could be an attractive therapy option.

Prostate-specific membrane antigen (PSMA) is a promising target for directing new therapies against several types of cancer. PSMA is a 750-amino acid type II transmembrane glycoprotein that is more avidly expressed in primary as well as in metastatic prostate cancer [5]. The level of PSMA expression on prostate cancer cells further increases with tumor dedifferentiation and in mCRPC, making it an ideal target for radionuclide therapy [6–9].

Recent studies have demonstrated the possibility of ^{177}Lu -PSMA-617 therapy as a viable treatment option in mCRPC [10,11]. The German Society of Nuclear Medicine recently published a multicenter retrospective case series for toxicity and PSA response in patients after ^{177}Lu -PSMA-617 treatment. The data showed a decline in the PSA level in 45% patients after all therapy cycles, and 40% patients already responded after a single cycle [12]. Small molecules, in general, are cleared very quickly from the circulation. Therefore, radiotherapy that is based on small molecules require high doses and frequent administrations, leading to systemic toxicity. To increase tumor accumulation and retention for radioligand therapy, and reduce dosage of ^{177}Lu , we conjugated a truncated Evans blue (EB) molecule and DOTA chelator onto PSMA-617 (EB-PSMA-617) and labeled it with ^{177}Lu . Preclinical studies showed high efficacy of ^{177}Lu -EB-PSMA in eradicating PSMA positive tumors [13]. This translational study is designed to assess the safety, dosimetry, and therapeutic response to a single, low-dose of ^{177}Lu -EB-PSMA-617 in comparison with ^{177}Lu -PSMA-617 in patients with mCRPC.

METHODS

Patients

This study was registered at clinicaltrials.gov (NCT03403595) and approved by the Institute Review Board of Peking Union Medical College Hospital, Chinese Academy of Medical Sciences and Peking Union Medical College. The following inclusion criteria were defined: all the patients had progressive metastatic castration-resistant prostate cancer that did not respond to androgen-suppression therapy and/or systemic chemotherapy. All patients had increasing blood PSA levels. Distant metastases with high PSMA expression were confirmed on ^{68}Ga -PSMA-617 PET/CT within one week before the injection of ^{177}Lu -EB-PSMA-617 or ^{177}Lu -PSMA-617. The exclusion criteria were a serum creatinine level of more than 150 $\mu\text{mol/L}$, a hemoglobin level of less than 10.0 g/dL, a white-cell count of less than $4.0 \times 10^9/\text{L}$, a platelet count of less than $100 \times 10^9/\text{L}$, a total bilirubin level of more than 60 $\mu\text{mol/L}$ (3 times the upper limit of the normal range) and a serum albumin level of more than 3.0 g/dL, cardiac insufficiency including carcinoid heart valve disease, a severe allergy or hypersensitivity to radiographic contrast material, and claustrophobia.

A total of 9 patients with mCRPC were recruited from November 2017 to February 2018 at Peking Union Medical College Hospital. The average patient age (mean \pm standard deviation) was 71 ± 5 years (range 60–81 years). Among the patients, 4 patients were in the ^{177}Lu -EB-PSMA-617 group and 5 patients were in the ^{177}Lu -PSMA-617 group (control group). The patients' basic characteristics are listed in Table 1.

^{68}Ga -PSMA-617 PET/CT imaging

Before and again at 1 month after the administration of ^{177}Lu -EB-PSMA-617 or ^{177}Lu -PSMA-617, all patients underwent ^{68}Ga -PSMA-617 whole-body PET/CT acquisitions (Siemens Medical Solutions, Erlangen, Germany) at 45–60 min after intravenous injection of about 1.85 MBq (0.05 mCi) per kilogram body weight of ^{68}Ga -PSMA-617 (85.10–125.80 GBq, 110.59 ± 12.88 GBq). Whole-body CT images were acquired using a low-dose CT scan (120 kV, 35 mA, 512×512 matrix, 3-mm layer, 70 cm field of view). The whole-body image of each patient was covered in 5–6 bed positions (2 min/bed), with the arms held above the head and from the proximal femur to the skull bottom.

For molecular response evaluation, we chose up to six lesions per patient with the highest ^{68}Ga -PSMA-617 uptakes in as many involved organ systems as possible as target lesions and calculated the percentage change of standardized uptake value calculated using body weight (SUV) after treatment relative to the baseline. Complete response (CR) was complete resolution of ^{68}Ga -PSMA-617 uptake in the target lesions. Partial response (PR) was defined as $>25\%$ decrease of the target lesions from the baseline scan, and $>25\%$ increase of the target lesions from the baseline scan was taken as progressive disease (PD). Neither CR, PR nor PD was considered stable disease (SD) that was $<25\%$ decrease or $<25\%$ increase of the target lesions from the baseline scan.

Radiopharmaceuticals

High-purity lutetium chloride was obtained from LuMark® (IDB, Holland). It was supplied as a sterile solution of $^{177}\text{LuCl}_3$ in 0.05 M HCl with the radionuclide purity of more than 99%. For radiolabeling, 3.7 GBq (100 mCi) of $^{177}\text{LuCl}_3$ was diluted with 0.3 mL of 0.5 M NH_4OAc (pH = 5.6), then EB-PSMA (200 μg dissolved in 10 μL absolute ethyl alcohol) or PSMA-617 (200 μg dissolved in 100 μL of metal-free water) was added. The mixture was heated for 30 min at 90 °C and then purified by C18 cartridge and passed through a 0.22- μm aseptic filtration membrane. Radiochemical purity control was performed with analytical thin-layer chromatography (Bioscan, USA). $\text{CH}_3\text{OH}:\text{NH}_4\text{OAc}$ (v/v 1:1) was used as the developing solution. The radiolabeling yield was greater than 90% and the radiochemical purity of $^{177}\text{Lu-PSMA-617}$ or $^{177}\text{Lu-EB-PSMA-617}$ was more than 95%.

Treatment Regime and Follow-up

Patients received intravenous hydration (2,000 mL of 0.9% NaCl; flow, 333 mL/h) starting 30 min before ^{177}Lu administration. The radiopharmaceutical diluted in 100 mL of physiological saline was co-administered slowly in an intravenous infusion for over 20–30 min. We used a single high level diagnostic dose for dosimetry calculation and evaluated the response. Four patients accepted intravenous injection with single dose 0.80–1.11 GBq (21.5–30 mCi) of $^{177}\text{Lu-EB-PSMA-617}$, the other 5 patients underwent single dose administration of $^{177}\text{Lu-PSMA-617}$ ranging from 1.30 to 1.42 GBq (35–38.4 mCi). To reduce therapy-induced damage to the salivary glands, the patients received ice packs over the parotid and submandibular glands starting from 30 min prior to and continued for 4 h after administration of $^{177}\text{Lu-EB-PSMA-617}$ or $^{177}\text{Lu-PSMA-617}$ [12]. Approximately 1–2 mL venous blood samples were collected at 20 min, 40 min, 60 min, 120 min, 1 d, 3 d, 5 d, and 7 d after injection from each patient in the $^{177}\text{Lu-EB-PSMA-617}$ group. Hematologic status, liver function, and renal function were documented before and every two weeks after the injection of $^{177}\text{Lu-EB-PSMA-617}$. The serum PSA response was documented monthly. Baseline and follow-up values of laboratory tests were classified into toxicity gradings using the Common Terminology Criteria for Adverse Events 3.0 [14].

SPECT/CT

Whole-body scintigraphy and SPECT/CT imaging were performed with a Philips Precedence scanner (Philips Healthcare, Andover, Massachusetts, USA), a medium-energy general-purpose collimator, a 20% energy window, a peak at 208 keV, a scan speed of 15 cm/min for whole-body imaging, and 32 frames with a 40 second exposure time per frame for each tomographic scan. Whole-body scintigraphy and SPECT/CT scans were acquired at different time points: 2, 24, 72, 120, and 168 h after injection of $^{177}\text{Lu-EB-PSMA-617}$; 0.5, 2, 24, 48, and 72 h after injection of $^{177}\text{Lu-PSMA-617}$.

Dosimetry Calculation

The dosimetry calculation was performed according to the European Association of Nuclear Medicine Dosimetry Guidance [15]. The OLINDA v1.1 software (Vanderbilt University, Nashville, Tennessee, USA) was used to derive absorbed doses of organs and whole-body effective dose. Two radioactive sources equipped with well-determined amounts of ^{177}Lu

activity were used to calculate dose concentration factor and voxel-based activity concentration which were converted to SUV in the volumes of interest. One radioactive source was a cylindrical phantom with a volume of 6.7 L and an internal diameter of 22 cm, which was homogeneously filled with a solution containing a total of 370 MBq ^{177}Lu activity to calculate the SUV of major organs. The other radioactive source was a cube phantom with a volume of 20 mL, which was homogeneously filled with a solution containing a total of 18.5 MBq ^{177}Lu activity to calculate the SUV of tumors. The decay uncorrected time-activity curve was generated based on the SUV of each organ or tissue. The SUV values were then converted to MBq/MBq using dose conversion factors based on organ weight from the adult male phantom by the OLINDA/EXM [16,17]. The number of disintegrations for the source organ was obtained using the OLINDA/EXM kinetic input model applying a monoexponential or a biexponential fit to the data of each source organ. The volume of left ventricle was set as 550 mL to calculate the residence of heart content. The ratio of activity mass concentrations for red marrow to blood was set as 0.32 to calculate dose delivery to bone marrow [18]. For organs such as salivary glands and tumors, which were not included in the OLINDA/EXM program, were assumed to have a morphology similar to that of a sphere and the absorbed doses were calculated in the sphere model program incorporated into the OLINDA software. The dimensions of the gland were estimated from direct measurement on CT images of the corresponding pretherapeutic ^{68}Ga -PSMA-617 PET/CT. The residence times of tumors were calculated by the trapezoidal method using Graphpad Prism (Version 4.0, GraphPad Software, Inc.) [19]. A total of 49 representative lesions (up to 6 tumor lesions per patient, same as the lesions used for molecular response evaluation) were analyzed (24 lesions for ^{177}Lu -EB-PSMA-617 and 25 lesions for ^{177}Lu -PSMA-617).

Statistical Analysis

Calculations were performed using SPSS software (IBM SPSS Statistics for Windows, Version 21.0; Armonk, NY). All quantitative data were expressed as mean \pm standard deviation. A *P* value of less than 0.05 was accepted as statistically significant. Two sample *t* tests were used to evaluate differences between the two groups. Correlations between SUVs, changes of SUV between pre- and post-therapeutic PET (SUV) and absorbed doses in tumor lesions were assessed using Spearman's rank correlation coefficient.

RESULTS

Safety

^{177}Lu -EB-PSMA-617 imaging dose was well tolerated by all 4 patients. No clinically significant adverse effects were reported or observed in any patient up to 3 months post injection. Out of 4 patients in the ^{177}Lu -EB-PSMA-617 group, one patient experienced Grade 1 leucopenia and anemia, and another patient developed grade 2 reduction in white blood cells. These two patients had been heavily pretreated with chemotherapy or ^{223}Ra -therapy of bone metastases and had an already-compromised bone marrow reserve before therapy. Nevertheless, both patients recovered within 8 weeks after injection of ^{177}Lu -EB-PSMA-617. Kidney function and liver function were not significantly changed within 2 months period of observation, *i.e.*, no significant change was observed in serum creatinine,

urea, alanine aminotransferase, aspartate transferase, glutamyl transpeptidase, and total bilirubin. No patient experienced relevant xerostomia, fatigue, nausea or loss of appetite during the first few weeks after therapy.

For the 5 patients subjected to ^{177}Lu -PSMA-617 therapy, no nephrotoxicity, hepatotoxicity, or hematological toxicity was observed. Fatigue was reported around 24–48 h after injection in 2 patients.

Pharmacokinetics

Normal physiological uptake of ^{177}Lu -EB-PSMA-617 was observed in the lacrimal glands, salivary glands, liver, intestines, spleen, kidneys and bladder. A representative example of ^{177}Lu -EB-PSMA-617 distribution is shown in Fig. 1. ^{177}Lu -EB-PSMA-617 had relatively long circulation with $t_{1/2\alpha}$ around 5.26 h and $t_{1/2\beta}$ around 143.9 h. Based on the quantitative data summarized in Table 2, ^{177}Lu -EB-PSMA-617 had much longer tumor residence time and higher tumor uptake than ^{177}Lu -PSMA-617. Excessive uptakes were still seen for multiple tumor lesions even at 168 h after injection of ^{177}Lu -EB-PSMA-617, while that of ^{177}Lu -PSMA-617 already dropped to almost the background level at 24 h p.i. Most of ^{177}Lu -EB-PSMA-617 in the lung, liver, kidneys, spleen, and muscle were also higher than those of ^{177}Lu -PSMA-617. The uptakes in the intestine were similar for the two agents.

Dosimetry for Normal Organs

Organ and effective doses of ^{177}Lu -EB-PSMA-617 and ^{177}Lu -PSMA-617 are given in Table 3. Whole body effective dose for ^{177}Lu -EB-PSMA-617 (0.1294 ± 0.0395 mSv/MBq) was higher than ^{177}Lu -PSMA-617 (0.0235 ± 0.0029 mSv/MBq, $P = 0.025$). The highest estimated radiation dose was calculated for parotid glands for both agents with 6.41 ± 1.40 mSv/MBq for ^{177}Lu -EB-PSMA-617 and 1.25 ± 0.51 mSv/MBq for ^{177}Lu -PSMA-617. For the kidneys, the calculated absorbed dose was 2.39 ± 0.69 mSv/MBq for ^{177}Lu -EB-PSMA-617 and 0.39 ± 0.06 mSv/MBq for ^{177}Lu -PSMA-617 ($P < 0.01$). ^{177}Lu -EB-PSMA-617 also had significantly higher effective dose in red bone marrow than ^{177}Lu -PSMA-617 (0.0547 ± 0.0062 vs. 0.0084 ± 0.0057 mSv/MBq, $P < 0.01$). As to effective dose in the small intestine, there was no significant difference between ^{177}Lu -EB-PSMA-617 and ^{177}Lu -PSMA-617 (0.31 ± 0.16 vs. 0.28 ± 0.21 mSv/MBq, $P = 0.82$).

Dosimetry for Tumor Lesions

Most of the lesions seen by ^{68}Ga -PSMA-617 PET were also visualized on ^{177}Lu -EB-PSMA-617 and ^{177}Lu -PSMA-617 planar images and SPECT. There was no significant difference in all the targeted tumor SUV values of ^{68}Ga -PSMA-617 between the disintegrations of all the tumors by mass average was 0.0766 ± 0.0385 MBq-h/MBq/g in patients receiving ^{177}Lu -EB-PSMA-617, which was about 2.15-fold higher than that in patients receiving ^{177}Lu -PSMA-617 (0.0356 ± 0.0361 MBq-h/MBq/g, $P < 0.001$).

In addition, the number of disintegrations of ^{177}Lu in the bone metastasis lesions in ^{177}Lu -EB-PSMA-617 group was about 5.68-fold higher than that in ^{177}Lu -PSMA-617 group (0.0766 ± 0.0385 MBq-h/MBq/g with 24 lesions vs. 0.0135 ± 0.0103 MBq-h/MBq/g with 15 lesions, $P < 0.001$) (Fig. 2). Similarly, SUV_{\max} of ^{68}Ga -PSMA-617 activity in bone lesions

was also found to be significantly higher in $^{177}\text{Lu-EB-PSMA-617}$ group (19.24 ± 14.45) than that in $^{177}\text{Lu-PSMA-617}$ group (6.50 ± 3.03 , $P < 0.001$).

When the bone tumors with comparable baseline SUV_{max} of $^{68}\text{Ga-PSMA-617}$ activity from 10.0–15.0 were selected from the two groups for comparison, the number of disintegrations in the bone metastasis lesions of $^{177}\text{Lu-EB-PSMA-617}$ group was about 3.02-fold higher than that in the $^{177}\text{Lu-PSMA-617}$ group (0.0575 ± 0.0214 MBq-h/MBq/g with 13 lesions vs. 0.0190 ± 0.0116 MBq-h/MBq/g with 8 lesions, $P < 0.001$).

Treatment Efficacy

Improvement in Clinical Symptoms—Out of the 4 patients received $^{177}\text{Lu-EB-PSMA-617}$ imaging dose, significant decrease in the severity of bone pain, with a reduction in visual analog scale scores from 7 before treatment to 4 after treatment was found in 1 patient. The pain intensity remained unchanged or slightly relieved in the other 3 patients, requiring constant use of analgetics. The Karnofsky Performance Status score improved in 2 patients, and no worsening was observed in any patient after radiopharmaceutical injection. In patients with $^{177}\text{Lu-PSMA-617}$ therapy, there was no change in clinical symptoms.

PSA Response.—In the $^{177}\text{Lu-EB-PSMA-617}$ therapy group, 2/4 patients demonstrated a reduction in PSA levels at 1 month after the treatment; in 1 patient the decrease was more than 50% and in 1 patient more than 20%. However, PSA level increase of 15% to 25% was noted in the remaining 2 patients with stable disease.

In 5 patients who underwent $^{177}\text{Lu-PSMA-617}$ injection, 1/5 patient showed a reduction in PSA level at 1 month after the treatment from 16.17 to 12.19 (25%). A PSA increase of greater than 50% was seen in 2 patients with progressive disease, an increase of less than 25% was noted in 2 patients with stable disease.

Molecular response.—Eight out of 9 patients underwent $^{68}\text{Ga-PSMA-617}$ PET/CT acquisition 1 month after the treatment. One patient in the $^{177}\text{Lu-EB-PSMA-617}$ therapy group failed to be checked due to constipation. In the $^{177}\text{Lu-EB-PSMA-617}$ group of 3 patients, the summed target lesions SUV_{max} decreased from 237, 71, and 86 to 113, 41, and 61, respectively ($\text{SUV} = -52\%$, -42% , and -29% , respectively). According to the criteria for response evaluation, all 3 patients subjected to low imaging dose $^{177}\text{Lu-EB-PSMA-617}$ therapy showed partial response (Fig. 3 A, B).

In the $^{177}\text{Lu-PSMA-617}$ group, 2 out of 5 patients showed decrease of summed target lesions SUV_{max} from 167 and 141 to 136 and 109, respectively ($\text{SUV} = -19\%$ and -23% , respectively), and the other 3 patients showed increase of summed SUV_{max} from 16, 43, and 27 to 16, 51, and 62 ($\text{SUV} = +3\%$, $+19\%$, and $+131\%$, respectively). Referring to the criteria, only 1 patient showed partial response (Fig. 3 C, D) and the other patients had SD.

When the tumors with comparable baseline SUV_{max} from 10.0–15.0 were selected from the two groups for comparison, the $^{177}\text{Lu-EB-PSMA-617}$ group showed significantly better tumor response than the control $^{177}\text{Lu-PSMA-617}$ group as demonstrated by SUV ($-32 \pm 0.14\%$, $n = 8$ vs. $0.21 \pm 0.37\%$, $n = 8$; $P = 0.002$).

Correlation of SUV and Absorbed Doses in Tumor Lesion

There was a moderate but highly statistically significant correlation between baseline SUV_{max} from ^{68}Ga -PSMA-617 PET/CT and the number of disintegrations in all the tumors for the ^{177}Lu -EB-PSMA-617 treatment ($r = 0.611$, $p = 0.002$). Change of SUV_{max} for all lesions showed a significantly negative correlation with the pretherapeutic SUV ($r = -0.550$, $P = 0.018$). No correlation could be found between the change of SUV_{max} and the number of disintegrations in all the tumors ($r = -0.164$, $P = 0.515$).

In addition, there was significant positive correlation between baseline SUV_{max} from ^{68}Ga -PSMA-617 PET/CT and the number of disintegrations in all the targeted tumors for the ^{177}Lu -PSMA-617 treatment ($r = 0.915$, $p < 0.001$). Change of SUV_{max} for all lesions showed negative correlation with the baseline SUV ($r = -0.582$, $P = 0.002$). Correlation was also found between the change of SUV_{max} and the number of disintegrations in all the tumors ($r = -0.558$, $P = 0.004$).

DISCUSSION

PSMA is overexpressed in almost all primary prostate tumors and metastases, offering an optimal target for various molecular-based radionuclide therapies in prostate cancer [20–22]. ^{177}Lu -J591, a monoclonal antibody probe that binds to the extracellular domain of PSMA, was first used for therapy but limited by myelosuppression. With the development of small-molecule PSMA ligands, ^{177}Lu -PSMA-617 has been increasingly used for radioligand therapy of mCRPC [19, 23–25]. Small-molecule ligands clear rapidly from blood circulation and therefore require large doses and/or repeated administration, which in turn may lead to unwanted toxicity to healthy organs and tissue. Hence, improving the pharmacokinetics of therapeutics in the blood has been regarded as a valuable means to reduce the number of injections and improve the efficacy of the drug. In prior studies, we synthesized ^{177}Lu -EB-PSMA-617 to increase the tumor accumulation and retention, and tested the compound in animal models and compared it to other albumin-binding moieties such as 4-iodophenyl butyric acid. In this first-in-human study, we present the data of safety, dosimetry and early response to single low dose (*i.e.* imaging dose) of ^{177}Lu -EB-PSMA-617 in patients with mCRPC, and comparison with ^{177}Lu -PSMA-617.

Due to albumin binding, longer intratumoral residence time of ^{177}Lu -EB-PSMA-617 compared to ^{177}Lu -PSMA-617, resulted in much higher absorbed doses in bone metastasis with comparable baseline SUV_{max} of 10.0–15.0. This result was consistent with the treatment response. At 1 month after the administration of low-dose ^{177}Lu -EB-PSMA-617, significant decrease of ^{68}Ga -PSMA-617 uptake was found which was not observed in the ^{177}Lu -PSMA-617 group. In addition to the decrease of ^{68}Ga -PSMA-617 uptake, all the patients that were re-evaluated 1 month after ^{177}Lu -EB-PSMA-617 injection showed partial response (three out of three), while only one patient out of five in the ^{177}Lu -PSMA-617 group showed partial response. This result suggests that ^{177}Lu -EB-PSMA-617 therapy will be more efficacious and may facilitate reduction of dose or dosing frequency.

Hematological toxicity is the most commonly reported adverse side effect related to ^{177}Lu PSMA therapy, especially for the patients with a heavy burden of skeletal metastases and

borderline marrow function. In men with significant bone metastases, up to 10–25% of men had a Grade 1–2 reduction in hemoglobin or platelets [26]. A multicenter retrospective case series for toxicity showed that 10%, 4%, and 3% of the patients experienced Grade 3–4 anemia, thrombocytopenia, and leukopenia, respectively [12]. In this study, $^{177}\text{Lu-EB-PSMA-617}$ showed relatively long half-life thus higher effective dose in red bone marrow than $^{177}\text{Lu-PSMA-617}$. In the current study, imaging dose of $^{177}\text{Lu-EB-PSMA-617}$ induced a reversible Grade 1–2 leucocyte reduction in 2 out of 4 patients with diffuse bone marrow involvement. A low blood count at baseline and extensive bone marrow infiltration in combination with previous chemotherapy or ^{223}Ra -therapy was considered a risk for the development of hematotoxicity [27,28]. Based on the mean absorbed dose to red marrow and dose limit of 2 Gy, similar patients can be injected with as much as 34 GBq of $^{177}\text{Lu-EB-PSMA-617}$. However, such therapeutic study should be carefully preformed with escalating doses and monitored closely.

Similar to $^{177}\text{Lu-PSMA-617}$, the highest estimated radiation dose of $^{177}\text{Lu-EB-PSMA-617}$ was observed in the kidneys and salivary glands. None of the current studies have reported nephrotoxicity. In our study, the calculated absorbed dose of $^{177}\text{Lu-EB-PSMA-617}$ was higher than $^{177}\text{Lu-PSMA-617}$. Kidney function (serum creatinine, urea) was not significantly changed within 2 months period of observation. However, monitoring closely renal function should be needed for further investigation with increased doses. Due to the high physiological uptake in healthy salivary glands, up to 30% of men reported dry mouth or xerostomia following high dose repeated $^{177}\text{Lu-PSMA-617}$ treatment [26]. Although salivary gland dysfunction is a common finding in patients treated with radioiodine, it is usually transient and persistent dysfunction rate was reported to be only 5% [29]. The salivary glands (parotid and submandibular glands) received the highest radiation dose of 6.41 ± 1.40 mSv/MBq for $^{177}\text{Lu-EB-PSMA-617}$. Although we did not observe xerostomia in patients with $^{177}\text{Lu-EB-PSMA-617}$ administration during follow-up, it is a matter of concern that increasing the dose might put the salivary glands at risk. A possible reduction of damage to salivary glands might be facilitated by applying icepacks to the glands in order to reduce blood flow and $^{177}\text{Lu-EB-PSMA-617}$ uptake during the blood pool phase.

$^{177}\text{Lu-EB-PSMA-617}$ allows the radioactivity to remain in the target, prolongs tumor retention, maximizes the therapeutic effect, and reduces dosage of ^{177}Lu , but also induces much higher estimated doses in other organs including several glands, kidneys and blood, increases potential side effects and especially hematotoxicity. To weigh the advantages and disadvantages, we are currently proposing a larger prospective study using 1.85 GBq (50 mCi)/cycle per patient with extensive bone marrow involvement and 3.70 GBq (100 mCi)/cycle per patient with predominant lymph node and soft tissue metastases.

There were several limitations in our study. Firstly, the most prominent of these is the small number of patients. Nevertheless, with this small cohort we observed that $^{177}\text{Lu-EB-PSMA-617}$ is significantly better than $^{177}\text{Lu-PSMA-617}$ and low imaging doses already achieved some therapeutic benefits to the patients. Secondly, our study lacked long-term observations of side effects such as nephrotoxicity and hepatotoxicity. Thirdly, it missed histological confirmation for CR. This study warrants future studies with escalating dose treatment of mCRPC patients. As suggested above, future studies with $^{177}\text{Lu-EB-}$

PSMA-617 patients with diffuse bone marrow involvement should be done carefully because these patients have a higher probability to develop hematotoxicity.

CONCLUSIONS

This first-in-human study demonstrates that ^{177}Lu -EB-PSMA-617 has much higher tumor accumulation than ^{177}Lu -PSMA-617 and a single imaging dose provides some therapeutic efficacy in patients with mCRPC. The ^{177}Lu -EB-PSMA-617 uptakes in kidneys and red bone marrow are higher than ^{177}Lu -PSMA-617 but are well tolerated at low doses. Further investigations with increased dose and frequency of administration are warranted.

Acknowledgments

Funding: This study was supported in part, by the Key Project on Inter-Governmental International Scientific and Technological Innovation Cooperation in National Key Projects of Research and Development Plan (2016YFE0115400), the Intramural Research Program (IRP), National Institute of Biomedical Imaging and Bioengineering (NIBIB), National Institutes of Health (NIH). This study was also partly supported by the Chinese Academy of Medical Science Major Collaborative Innovation Project (2016-12M-1-011), Welfare Research Funding for Public Health Professionals (201402001), National Nature Science Foundation (81741142) and Beijing Municipal Natural Science Foundation (7161012).

REFERENCES

- [1]. Siegel RL, Miller KD, Jemal A. Cancer Statistics, 2017. *CA Cancer J Clin*, 2017;67(1):7–30. [PubMed: 28055103]
- [2]. Kirby M, Hirst C, Crawford ED. Characterising the castration-resistant prostate cancer population: a systematic review. *Int J Clin Pract*. 2011;65:1180–1192. [PubMed: 21995694]
- [3]. Cornford P, Bellmunt J, Bolla M, et al. EAU-ESTRO-SIOG guidelines on PC. Part II: treatment of relapsing, metastatic, and CRPC. *Eur Urol*. 2017;71:630–42. [PubMed: 27591931]
- [4]. Heidenreich A, Bastian PJ, Bellmunt J, et al. EAU guidelines on prostate cancer. Part 1: screening, diagnosis, and local treatment with curative intent—update 2013. *Eur Urol*. 2014;65:124–137. [PubMed: 24207135]
- [5]. Rajasekaran AK, Anilkumar G, Christiansen JJ. Is prostate specific membrane antigen a multifunctional protein? *Am J Physiol Cell Physiol* 2005; 288: C975–81. [PubMed: 15840561]
- [6]. Ghosh A and Heston WD. Tumor target prostate specific membrane antigen (PSMA) and its regulation in prostate cancer. *J Cell Biochem*. 2004; 91:528–539. [PubMed: 14755683]
- [7]. Perner S, Hofer MD, Kim R, et al. Prostate-specific membrane antigen expression as a predictor of prostate cancer progression. *Hum Pathol*. 2007;38:696–701. [PubMed: 17320151]
- [8]. Afshar-Oromieh A, Malcher A, Eder M, et al. PET imaging with a [^{68}Ga]gallium-labelled PSMA ligand for the diagnosis of PCa: biodistribution in humans and first evaluation of tumour lesions. *Eur J Nucl Med Mol Imaging* 2013; 40:486–495. [PubMed: 23179945]
- [9]. Wright GL, Jr, Haley C, Beckett ML, et al. Expression of prostate-specific membrane antigen in normal, benign, and malignant prostate tissues. *Urol Oncol* 1995; 1: 18–28. [PubMed: 21224086]
- [10]. Benesová M, Schafer M, Bauder-Wust U, et al. Preclinical evaluation of a tailor made DOTA-conjugated PSMA inhibitor with optimized linker moiety for imaging and endoradiotherapy of prostate cancer. *J Nucl Med* 2015; 56:914–920. [PubMed: 25883127]
- [11]. Yadav MP, Ballal S, Tripathi M, et al. ^{177}Lu -DKFZ-PSMA-617 therapy in metastatic castration resistant prostate cancer: Safety, efficacy, and quality of life assessment. *Eur J Nucl Med Mol Imaging* 2016; 44: 81–91. [PubMed: 27506431]
- [12]. Rahbar K, Ahmadzadehfard H, Kratochwil C, et al. German multicenter study investigating ^{177}Lu -PSMA-617 radioligand therapy in advanced prostate cancer patients. *J Nucl Med*. 2017;58(1): 85–90. [PubMed: 27765862]

- [13]. Jacobson O, Wang Z, Niu G, Ma Y, Kiesewetter DO, Chen X. A single injection of Evans blue modified ^{177}Lu -PSMA-617 provides a radiotherapeutic cure for prostate-specific membrane antigen (PSMA) tumor xenografts in mice. *J Nucl Med* 2018; abstract in press.
- [14]. Common Terminology Criteria for Adverse Events v3.0 (CTCAE). cancer.gov Website. http://ctep.cancer.gov/protocolDevelopment/electronic_applications/docs/ctcae_v3.pdf. Published August 9, 2006. Accessed April 14, 2016.
- [15]. Lassmann M, Chiesa C, Flux G, Bardies M. EANM Dosimetry Committee guidance document: good practice of clinical dosimetry reporting. *Eur J Nucl Med Mol Imaging*. 2011;38:192–200. [PubMed: 20799035]
- [16]. Roivainen A, Kähkönen E, Luoto P, et al. Plasma pharmacokinetics, whole-body distribution, metabolism, and radiation dosimetry of ^{68}Ga bombesin antagonist BAY 86–7548 in healthy men. *J Nucl Med*. 2013;54:867–872. [PubMed: 23564761]
- [17]. Wang Z, Zhang M, Wang L, et al. Prospective study of ^{68}Ga -NOTA-NFB: radiation dosimetry in healthy volunteers and first application in glioma patients. *Theranostics*. 2015;5:882–889. [PubMed: 26000059]
- [18]. Wessels BW, Bolch WE, Bouchet LG, et al. Bone marrow dosimetry using blood-based models for radiolabeled antibody therapy: a multiinstitutional comparison. *J Nucl Med*. 2004;45:1725–1733. [PubMed: 15471841]
- [19]. Kratochwil C, Giesel FL, Stefanova M, et al. PSMA-targeted radionuclide therapy of metastatic castration-resistant prostate cancer with Lu-177 labeled PSMA-617. *J Nucl Med*. 2016;57:1170–1176. [PubMed: 26985056]
- [20]. Minner S, Wittmer C, Graefen M, et al. High level PSMA expression is associated with early PSA recurrence in surgically treated prostate cancer. *Prostate* 2011;71:281–288. [PubMed: 20809553]
- [21]. Rybalov M, Ananias HJ, Hoving HD, et al. PSMA, EpCAM, VEGF and GRPR as imaging targets in locally recurrent prostate cancer after radiotherapy. *Int J Mol Sci* 2014; 15:6046–6061. [PubMed: 24727373]
- [22]. Ananias HJ, van den Heuvel MC, Helfrich W, et al. Expression of the gastrin-releasing peptide receptor, the prostate stem cell antigen and the prostate-specific membrane antigen in lymph node and bone metastases of prostate cancer. *Prostate* 2009; 69:1101–1108. [PubMed: 19343734]
- [23]. Ahmadzadehfard H, Eppard E, Kurpig S, et al. Therapeutic response and side effects of repeated radioligand therapy with ^{177}Lu -PSMA-DKFZ-617 of castrate-resistant metastatic prostate cancer. *Oncotarget*. 2016;7:12477–12488. [PubMed: 26871285]
- [24]. Rahbar K, Schmidt M, Heinzl A, et al. Response and tolerability of a single dose of ^{177}Lu -PSMA-617 in patients with metastatic castration-resistant prostate cancer: a multicenter retrospective analysis. *J Nucl Med*. 2016;57:1334–1338. [PubMed: 27056618]
- [25]. Rahbar K, Bode A, Weckesser M, et al. Radioligand therapy with ^{177}Lu -PSMA-617 as a novel therapeutic option in patients with metastatic castration resistant prostate cancer. *Clin Nucl Med*. 2016;41:522–528. [PubMed: 27088387]
- [26]. Emmett L, Willowson K, Violet J, et al. Lutetium ^{177}Lu PSMA radionuclide therapy for men with prostate cancer: a review of the current literature and discussion of practical aspects of therapy. *J Med Radiat Sci*. 2017 3;64(1):52–60. [PubMed: 28303694]
- [27]. Kulkarni HR, Singh A, Schuchardt C, et al. PSMA-based radioligand therapy for metastatic castration-resistant prostate cancer: the Bad Berka experience since 2013. *J Nucl Med*. 2016;57(Suppl 3):97S–104S. [PubMed: 27694180]
- [28]. Delker A, Fendler WP, Kratochwil C, et al. Dosimetry for Lu-DKFZ-PSMA-617: a new radiopharmaceutical for the treatment of metastatic prostate cancer. *Eur J Nucl Med Mol Imaging*. 2016;43:42–51. [PubMed: 26318602]
- [29]. Jeong SY, Kim HW, Lee SW, Ahn BC, Lee J. Salivary gland function 5 years after radioactive iodine ablation in patients with differentiated thyroid cancer: direct comparison of pre- and postablation scintigraphies and their relation to xerostomia symptoms. *Thyroid*, 2013;23:609–616. [PubMed: 23153322]

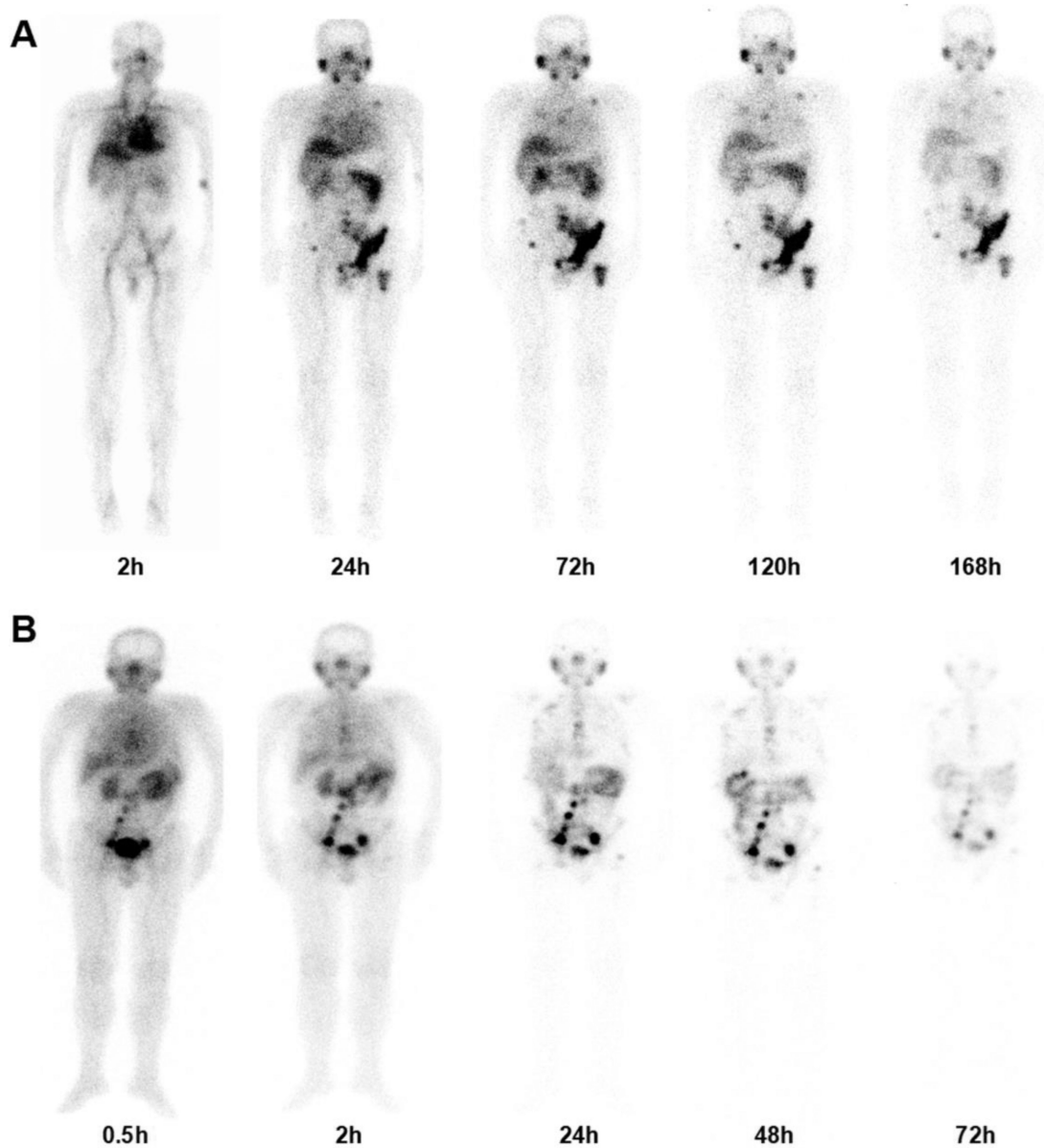
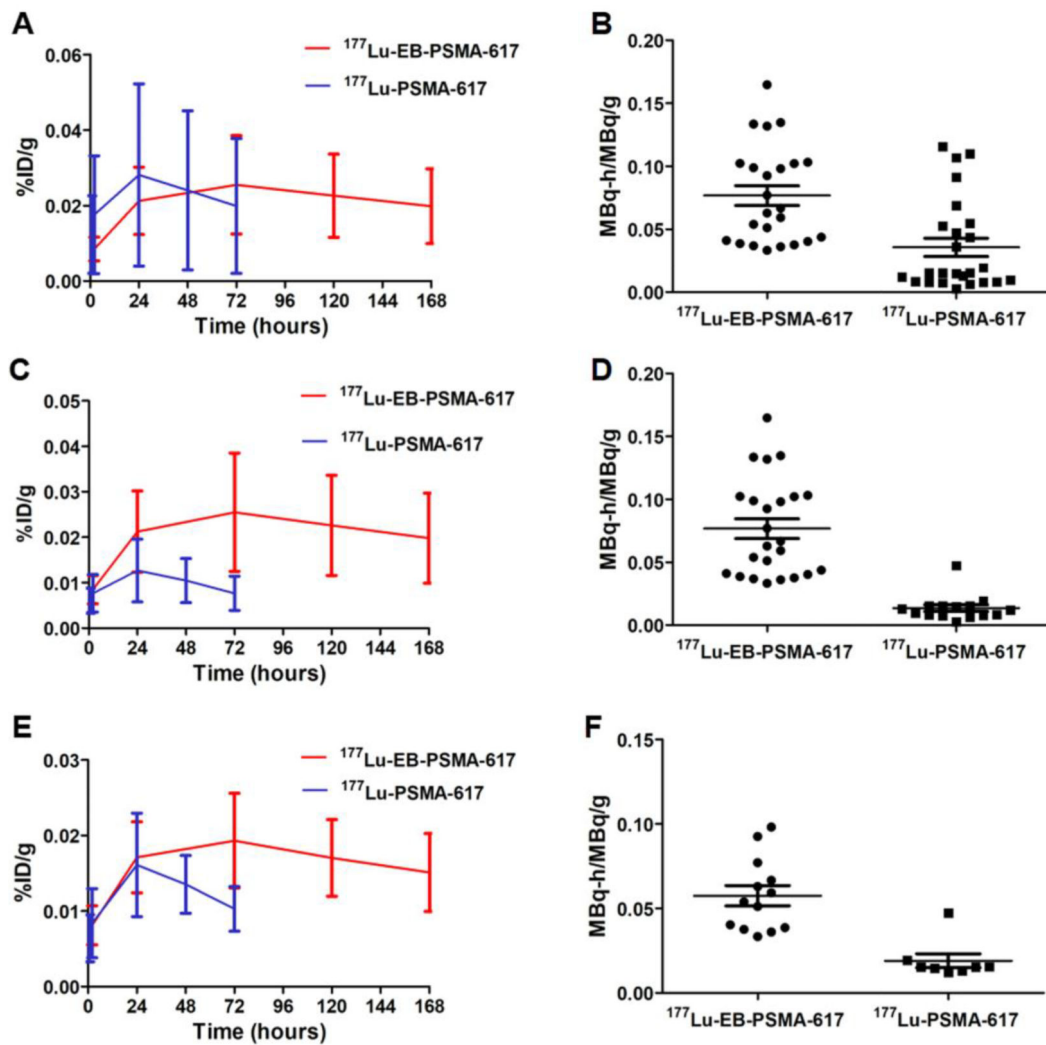


FIGURE 1.

(A) Representative whole-body anterior projection images of a 70-y-old male patient with mCRPC at different time points after intravenous administration of $^{177}\text{Lu-EB-PSMA-617}$.

(B) Representative whole-body anterior projection images of a 72-y-old male patient with mCRPC at different time points after intravenous administration of $^{177}\text{Lu-PSMA-617}$.

**FIGURE 2.**

Time-activity curves and number of disintegrations of all the lesions (A, B), all the bone lesions (C, D) and the bone tumors with comparable baseline SUV_{max} of $^{68}\text{Ga-PSMA-617}$ activity from 10.0–15.0 after administration of $^{177}\text{Lu-EB-PSMA-617}$ (red) and $^{177}\text{Lu-PSMA-617}$ (blue).

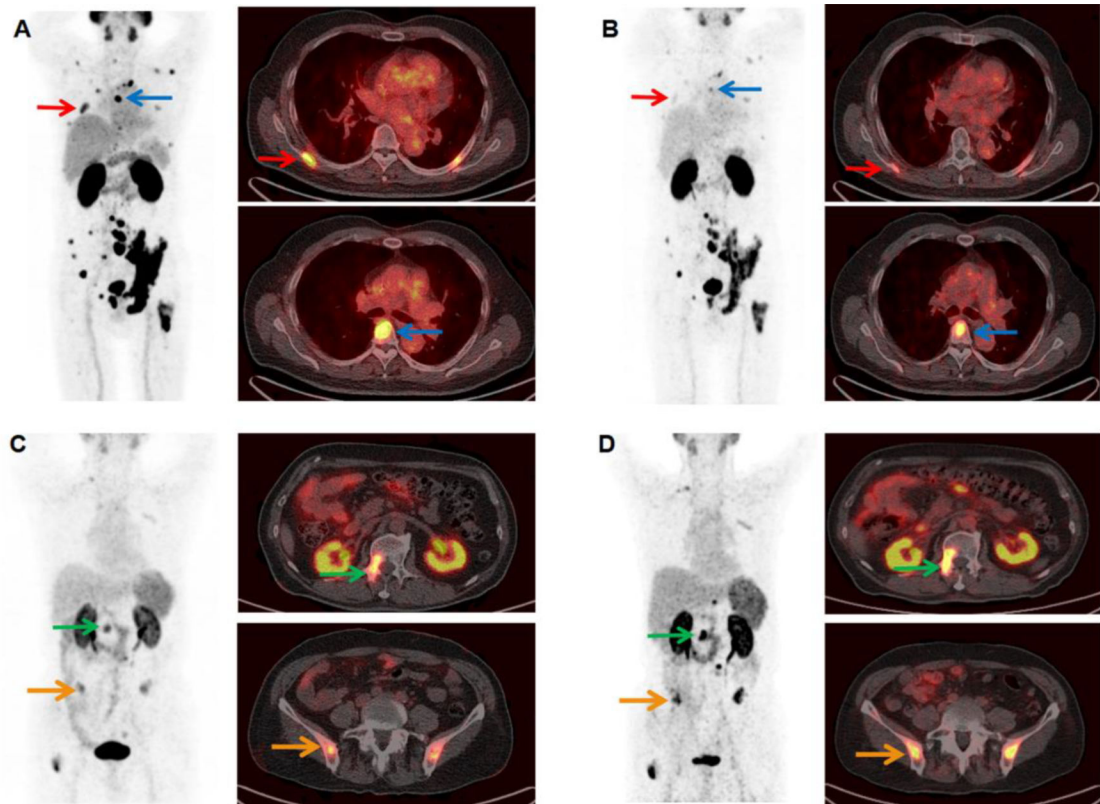


FIGURE 3.

Comparison of ^{68}Ga -PSMA-617 PET/CT images immediately before (A) and 1 month after (B) injection of 1.11 GBq (30.0 mCi) of ^{177}Lu -EB-PSMA-617 in a patient (patient 1) with mCRPC. The SUV_{max} of the right scapula decreased from 10 to 3 (red arrow), and the SUV_{max} of bone metastasis in T6 decreased from 21 to 7 (blue arrow). Comparison of ^{68}Ga -PSMA-617 PET/CT images immediately before (C) and 1 month after (D) injection of 1.27GBq (34.30 mCi) of ^{177}Lu -PSMA-617 in a patient (patient 7) with mCRPC. The SUV_{max} of bone metastasis in S1 increased from 5 to 12 (green arrow), and the SUV_{max} of the right ilium increased from 4 to 8 (yellow arrow).

Table 1.

Basic characteristics of the enrolled patients

Patient No.	Age	Gleason	Previous therapies										metastasis	Treatment agent	Dose (GBq)
			Prostatectomy	External-beam radiation therapy	Chemotherapy	²²³ Ra	LHRH analogs	Bicalu	Abirat	Enzalu					
1	70	4+5	N	N	Y	N	Y*	N	N	Y	N	Y	BN	¹⁷⁷ Lu-EB-PSMA-617	1.11
2	73	4+5	Y	N	Y	N	N	N	Y	Y	Y*	Y*	BN	¹⁷⁷ Lu-EB-PSMA-617	1.09
3	76	4+4	Y	Y	Y	Y	Y*	Y*	N	Y	Y	N	BN	¹⁷⁷ Lu-EB-PSMA-617	0.83
4	70	3+4	Y	Y	Y	N	Y*	Y*	Y	Y*	N	N	BN	¹⁷⁷ Lu-EB-PSMA-617	0.77
5	60	4+4	N	N	Y	N	Y*	Y*	Y*	N	N	N	BN	¹⁷⁷ Lu-PSMA-617	1.30
6	81	3+5	Y	Y	N	N	Y*	Y*	Y	Y	Y	N	BN	¹⁷⁷ Lu-PSMA-617	1.30
7	70	5+5	N	Y	Y	N	Y*	Y*	Y	Y	Y	Y	BN	¹⁷⁷ Lu-PSMA-617	1.27
8	72	4+5	N	Y	Y	N	Y*	Y*	Y	Y	Y	Y*	BN, LN	¹⁷⁷ Lu-PSMA-617	1.39
9	67	5+5	Y	Y	N	N	N	N	Y	Y	Y	Y*	BN, LN	¹⁷⁷ Lu-PSMA-617	1.42

LHRH: luteinizing hormone-releasing hormone; Bicalu: Bicalutamide; Abirat: Abiraterone; Enzalu: Enzalutamide; BN: bone; LN: lymph node.

* The hormone therapies were not discontinued despite refractory situation according to the continuing PSA elevation under these medications.

Table 2. Biodistribution of ^{177}Lu -EB-PSMA-617 and ^{177}Lu -PSMA-617 in patients with mCRPC.

Organ	^{177}Lu -EB-PSMA-617(SUV \pm SD, n = 4)				^{177}Lu -PSMA-617 (SUV \pm SD, n = 5)					
	2 h	24 h	72 h	120 h	168 h	0.5 h	2 h	24 h	48 h	72 h
Blood	7.21 \pm 1.25	1.87 \pm 0.60	1.24 \pm 0.41	0.88 \pm 0.23	0.67 \pm 0.10	2.53 \pm 0.69	1.66 \pm 0.36	0.29 \pm 0.07	0.08 \pm 0.02	0.05 \pm 0.04
Lungs	0.94 \pm 0.09	0.56 \pm 0.10	0.44 \pm 0.19	0.41 \pm 0.19	0.43 \pm 0.19	0.73 \pm 0.16	0.58 \pm 0.15	0.15 \pm 0.02	0.08 \pm 0.03	0.04 \pm 0.01
Liver	4.82 \pm 0.91	2.84 \pm 0.77	2.53 \pm 1.00	2.59 \pm 0.88	2.52 \pm 0.99	3.36 \pm 1.04	2.99 \pm 0.87	1.48 \pm 0.44	0.66 \pm 0.19	0.38 \pm 0.17
Spleen	5.67 \pm 0.62	3.89 \pm 1.00	3.28 \pm 1.41	2.88 \pm 1.31	2.47 \pm 0.80	4.69 \pm 1.88	4.07 \pm 1.90	1.15 \pm 0.76	0.50 \pm 0.31	0.23 \pm 0.15
Pancreas	2.29 \pm 0.54	1.42 \pm 0.33	0.98 \pm 0.49	0.90 \pm 0.24	0.52 \pm 0.07	1.37 \pm 0.20	0.87 \pm 0.18	0.28 \pm 0.17	0.19 \pm 0.16	0.09 \pm 0.07
Kidneys	4.97 \pm 0.54	6.85 \pm 1.46	7.76 \pm 0.37	7.38 \pm 2.26	5.70 \pm 1.38	9.18 \pm 3.53	8.79 \pm 4.29	5.41 \pm 1.35	2.59 \pm 0.21	1.57 \pm 0.55
Muscle	0.52 \pm 0.17	0.37 \pm 0.13	0.26 \pm 0.08	0.28 \pm 0.1	0.24 \pm 0.12	0.66 \pm 0.13	0.40 \pm 0.04	0.08 \pm 0.02	0.01 \pm 0.01	0.00 \pm 0.00
Stomach	1.33 \pm 0.17	0.68 \pm 0.20	0.64 \pm 0.23	0.42 \pm 0.22	0.27 \pm 0.12	0.91 \pm 0.28	0.76 \pm 0.22	0.24 \pm 0.14	0.12 \pm 0.07	0.04 \pm 0.03
Intestine	0.94 \pm 0.28	1.39 \pm 0.50	1.25 \pm 0.84	1.24 \pm 0.79	0.98 \pm 0.49	1.57 \pm 0.37	1.57 \pm 0.82	2.30 \pm 0.65	1.62 \pm 1.10	0.85 \pm 0.76
Tumor	5.78 \pm 2.01	16.44 \pm 7.65	24.84 \pm 13.87	27.33 \pm 15.26	28.93 \pm 16.55	8.31 \pm 6.39	11.72 \pm 9.51	20.53 \pm 16.48	19.41 \pm 16.06	17.62 \pm 15.29

Table 3.Estimated effective dose after intravenous administration of $^{177}\text{Lu-EB-PSMA-617}$ and $^{177}\text{Lu-PSMA-617}$

Target organ	$^{177}\text{Lu-EB-PSMA}$ (mSv/MBq)	$^{177}\text{Lu-PSMA}$ (mSv/MBq)
Adrenals	0.0200 ± 0.0040	0.0031 ± 0.0007
Brain	0.0008 ± 0.0002	0.0001 ± 0.0000
Breasts	0.0039 ± 0.0006	0.0005 ± 0.0001
Gallbladder Wall	0.0248 ± 0.0057	0.0048 ± 0.0020
LLI Wall	0.0068 ± 0.0020	0.0021 ± 0.0012
Small Intestine	0.3123 ± 0.1644	0.2776 ± 0.2052
Stomach Wall	0.0446 ± 0.0086	0.0098 ± 0.0026
ULI Wall	0.0129 ± 0.0035	0.0049 ± 0.0029
Heart Wall	0.3993 ± 0.0283	0.0504 ± 0.0231
Kidneys	2.3875 ± 0.6929	0.3948 ± 0.0610
Liver	0.8498 ± 0.2428	0.1478 ± 0.0715
Lungs	0.1550 ± 0.0461	0.0164 ± 0.0037
Muscle	0.0979 ± 0.0265	0.0072 ± 0.0018
Ovaries	0.0086 ± 0.0026	0.0031 ± 0.0019
Pancreas	0.3163 ± 0.0573	0.0349 ± 0.0153
Red Marrow	0.0547 ± 0.0062	0.0084 ± 0.0057
Osteogenic Cells	0.0320 ± 0.0032	0.0047 ± 0.0028
Skin	0.0031 ± 0.0006	0.0004 ± 0.0001
Spleen	0.8208 ± 0.1342	0.1143 ± 0.0602
Testes	0.0032 ± 0.0009	0.0003 ± 0.0001
Thymus	0.0072 ± 0.0010	0.0008 ± 0.0002
Thyroid	0.0041 ± 0.0010	0.0003 ± 0.0001
Urinary Bladder Wall	0.0102 ± 0.0041	0.0163 ± 0.0150
Uterus	0.0081 ± 0.0025	0.0029 ± 0.0017
Total Body	0.0828 ± 0.0151	0.0123 ± 0.0035
Effective Dose Equivalent	0.3210 ± 0.0608	0.0635 ± 0.0173
Effective Dose	0.1294 ± 0.0395	0.0235 ± 0.0029
Salivary glands	6.4100 ± 1.4000	1.2500 ± 0.5100

LLI: Lower large intestine; ULI: Upper large intestine.